Eur Radiol (2016) 26:3978–3988
DOI 10.1007/s00330-016-4232-7

MAGNETIC RESONANCE

Alterations of diffusion tensor MRI parameters in the brains of patients with Parkinson's disease compared with normal brains: possible diagnostic use

Chin-Song Lu[1,2,3] · Shu-Hang Ng[4,5] · Yi-Hsin Weng[1,2,3] · Jur-Shan Cheng[6] · Wey-Yil Lin[1,2,3] · Yau-Yau Wai[7] · Yao-Liang Chen[4,7] · Jiun-Jie Wang[2,4,5,8]

Received: 14 September 2015 / Revised: 12 January 2016 / Accepted: 20 January 2016 / Published online: 5 March 2016

Abstract

Objectives To investigate the diagnostic performance of diffusion tensor imaging in patients with Parkinson's disease (PD).

Methods We examined a total of 126 PD patients (68 males/58 females, mean age: 62.0 ±7.6 years) and 91 healthy controls (43 males/48 females, mean age: 59.8 ±7.2 years). Images were acquired on a 3 Tesla magnetic resonance scanner. The Camino software was used to normalize and parcellate diffusion-weighted images into 90 cerebral regions based on the automatic anatomical labelling template. The minimum, median, and maximum values of the mean/radial/axial diffusivity/fractional anisotropy were determined. The diagnostic performance was assessed by receiver operating characteristic analysis. The associations of imaging parameters with disease severity were tested using Pearson's correlation coefficients after adjustment for disease duration.

Results Compared with healthy controls, PD patients showed increased diffusivity in multiple cortical regions that extended beyond the basal ganglia. An area under curve of 85 % was identified for the maximum values of mean diffusivity in the ipsilateral middle temporal gyrus. The most significant intergroup difference was 26.8 % for the ipsilateral inferior parietal gyrus.

Conclusion The measurement of water diffusion from the parcellated cortex may be clinically useful for the assessment of PD patients.

Key Points

- *Increased diffusivity was identified in multiple cortical regions of Parkinson's disease patients.*
- *The area under the receiver operating curve was 85 % in the middle temporal gyrus.*
- *The ipsilateral inferior parietal gyrus showed the most significant change.*

Keywords Parkinson's disease · Diffusion tensor imaging · Computer assisted diagnosis · Temporal gyrus · Parietal lobule

Chin-Song Lu and Shu-Hang Ng contributed equally to this work.

Electronic supplementary material The online version of this article (doi:10.1007/s00330-016-4232-7) contains supplementary material, which is available to authorized users.

✉ Jiun-Jie Wang
jwang@mail.cgu.edu.tw

1 Division of Movement Disorders,Department of Neurology, Chang Gung Memorial Hospital, Taoyuan, Taiwan

2 Neuroscience Research Center, Chang Gung Memorial Hospital, Taoyuan, Taiwan

3 School of Traditional Chinese Medicine, Chang Gung University, Taoyuan, Taiwan

4 Department of Medical Imaging and Intervention, Chang Gung Memorial Hospital, Linkou, Taiwan

5 Department of Medical Imaging and Radiological Sciences, Chang Gung University, 259 WenHua 1st Road, Taoyuan County 333, Taiwan

6 Clinical Informatics and Medical Statistics Research Center,College of Medicine, Chang Gung University, Taoyuan, Taiwan

7 Department of Medical Imaging and Intervention, Chang Gung Memorial Hospital, Keelung, Taiwan

8 Medical Imaging Research Center, Institute for Radiological Research, Chang Gung University / Chang Gung Memorial Hospital, Linkou, Taoyuan, Taiwan

Introduction

Parkinson's disease (PD) − a progressive neurodegenerative disorder which causes tremor at rest, bradykinesia, and postural instability − results from the massive loss of dopaminergic neurons in the substantia nigra pars compacta along with the

occurrence of Lewy bodies [1, 2]. The diagnosis of PD remains clinical. However, the accuracy of the clinical diagnosis remains as low as 53 % when the disease duration is less than 5 years and the neuropathological criteria are used as the gold standard [3]. Magnetic resonance imaging (MRI) examinations are generally performed to rule out concomitant disorders rather than for diagnostic confirmation. Although image-based volumetric measurements have been previously performed [4–6], volumetric loss is not specific to PD and can be evident only in advanced disease stages. Therefore, a non-invasive, ionizing radiation-free diagnostic imaging biomarker of PD would be highly desirable.

Diffusion tensor imaging (DTI) has been extensively utilized to study neurodegenerative diseases [7–12]. Several metrics can be derived from diffusion tensor imaging, including fractional anisotropy (FA), as well as mean, radial, and axial diffusivity (MD, RD, and AD, respectively). The use of DTI in patients with PD has been chiefly limited to hypothesis-driven selection of specific regions of interest (ROIs) in the basal ganglia [1, 2, 13] or focuses on white matter lesions. Villaincourt et al. [14] have previously shown a reduced FA in the caudal part of the substantia nigra in patients with PD, although a large overlap with values observed in healthy subjects was evident [15, 16]. In contrast, a large prospective study failed to identify significant differences in MD values between patients and controls [17].

The change of the measured diffusivity is frequently related to a shift of water balance between different compartments. Because water could be restricted or hindered by the organelle or membrane, the measured water diffusivity could be increased if the extracellular contribution is dominant, as a result of potential cell death or shrinkage. Most ROI-based analyses published to date focused on mean values of DTI. However, recent studies in the field of oncology have reported more pronounced changes from the minimum value rather than the average [18, 19]. In this prospective study, we hypothesized that the minimum, mean, and maximum MD values could be altered in PD patients compared with healthy subjects.

To obtain unbiased results with respect to the current pathophysiological model of PD, systematic DTI investigations of different brain regions are required. Recent technical advances in DTI have allowed spatial normalization of whole-brain images using reverse-affine transformation to maintain the quality of the principal diffusion direction [20, 21] through the use of specific software applications (e.g., Camino) [22]. Furthermore, there is evidence suggesting that both glutamate and glutamine levels are increased in the lentiform nucleus of patients with early-stage PD [23]. These findings are in line with the observation that >50 % of all dopaminergic neurons in the nigrostriatal projection are lost before the onset of PD. If disease severity and diffusion index are correlated with each other, DTI can be useful to assess the response to therapeutic interventions (especially in patients with early-stage disease).

In the current study, we sought to identify the cerebral regions and the diffusion indexes with the best diagnostic performance in PD patients. Subsequently, the percentage change of diffusion between PD patients and healthy controls was compared. Finally, we examined the correlations between the diffusion index and the disease severity. The overall goal was to investigate the regional changes of diffusion tensor throughout the brains of PD patients.

Materials and methods

The study protocol followed the tenets of the Declaration of Helsinki and was reviewed and approved by the local Institutional Review Board. All subjects provided their written informed consent to participate after a detailed explanation of the study.

Participants

This is a case-control study with a prospective design. A total of 126 patients with PD (68 males, mean age: 62.0 ±7.6 years; mean disease duration: 8.2 ±6.1 years) and 91 healthy control subjects (43 males, mean age: 59.8 ±7.2 years) were enrolled. All patients met the National Institute of Neurological Disorders and Stroke diagnostic criteria [24] for probable PD, the only exception being age at onset. To avoid the confounding effects of drugs, all of the anti-parkinsonian medications were withdrawn at least 12 h before assessing the severity of motor disability. We determined for each patient the Schwab and England Activities of Daily Living (ADL: 80.3 ±17.8) scale, the Unified Parkinson Disease Rating Scale (UPDRS: 35.5 ±23.4, the motor subscale: 21.9 ±14.3), modified Hohen and Yahr (mHY: 2.3 ±1.2) staging, and Mini-Mental State Examination (MMSE: 27.4 ±2.9). All controls underwent a thorough review of medical history and a careful physical examination, including a full neurological exam and MMSE (29.1 ±1.1). Patients were excluded in presence of the following criteria: 1) presence of brain abnormalities (including hydrocephalus or encephalomalacia) that may impair cognitive function on imaging studies (MRI and/or ^{18}FDG-PET), 2) history of intracranial surgery (including thalamotomy, pallidotomy, and/or deep brain stimulation), or 3) major physical or neuropsychiatric disorders. Patients with mild cortical atrophy were deemed eligible.

Image acquisition

Images were acquired on a 3 Tesla (T) MRI scanner (MAGNETOM Trio, Siemens, Erlangen, Germany) using a 12-channel head matrix coil. The patient's head was held still by a fixation pad during the scanning session in order to reduce bulk motion. Conventional imaging (i.e., T2-weighted

turbo spin-echo, T2-weighted FLAIR, and T1-weighted MP-RAGE sequences) was performed to rule out concomitant neurological disorders (e.g., stroke, moderate-to-severe dementia and severe dyskinesia). The imaging parameters for T1-weighted images were as follows: repetition time (TR)/echo time (TE)/inversion time (TI)/flip angle = 2000 ms/2.63 ms/900 ms/9°, slice thickness = 1 mm, number of slices = 160, matrix size = 224 × 256, and field of view (FOV) = 224 × 256 mm. The acquisition time was 4 min 08 sec. DTI images were acquired using an spin-echo echo planar imaging sequence with the following parameters: TR/TE/slice thickness = 5700 ms/108 ms/3 mm, matrix size = 96 × 96, and FOV = 192 × 192 mm. Parallel imaging was used, with an acceleration factor of two and generalized autocalibrating partially parallel acquisition (GRAPPA) reconstruction. Thirty slices were acquired covering the entire brain with a b-value of 1000 s/mm^2. Diffusion-weighting gradients were applied in 30 non-collinear directions. An additional non-diffusion-weighted image was also acquired.

Image post-processing

A voxel-based morphometry analysis was performed using high-resolution T1-weighted MP-RAGE images according to the standard procedure [25]. We then performed whole-brain parcellation with the Camino software (http://cmic.cs.ucl.ac.uk/camino/) [26] using the recommended procedures and parameters. Individual FA values were normalized to the standard ICBM-152 template from the International Consortium for Brain Mapping. The brain was subsequently parcellated into 116 areas as specified in the AAL template. The normalization parameters were subsequently applied to the MD map. A parenchyma mask was created by segmentation on the non-diffusion-weighted image, which was subsequently applied on all the maps of diffusion index [with the goal of reducing the impact of cerebrospinal fluid (CSF)]. We then calculated the 10th (minimum), 50th (median), and 90th (maximum) percentiles of diffusion index for each parcellated brain region. After the exclusion of 26 cerebellar regions, a total of 90 cerebral regions were included in the final analysis. The extracted values from the ROIs were then reorganized in each patient taking into account the laterality of disease onset.

Statistical analysis

The sensitivity, specificity, and optimal cut-off points of the diffusion tensor for differentiating patients with PD from controls were calculated using receiver operating characteristic (ROC) analyses. The area under the ROC curve (AUC) provides a measure of the overall discriminative ability of a variable for each region of interest. The differences in diffusion index were compared using the Student's *t* test. When statistically significant differences were detected, we calculated the percentage changes between average values of PD patients and healthy controls. Disease severity was expressed with the following parameters: disease duration, ADL, total and motor subscale of UPDRS, and MMSE. The associations between disease severity and the diffusion tensor index were investigated using Pearson's correlation coefficients after adjustment for disease duration. All calculations were performed using the SPSS software package, version 18.0 (SPPS Inc., Chicago, IL, USA). Two-tailed P values < 0.000138 (after correction for multiple comparisons) were considered statistically significant.

Results

Figure 1 shows two axial images of MD — located in the middle temporal lobe (A) and inferior parietal lobe (B) — from one representative patient. The images were overlapped with the corresponding AAL template (C and D, respectively).

Diagnostic performance of diffusion tensor

Table 1 reports the minimum, median, and maximum values of diffusion index for different brain areas of PD patients and healthy controls. Both the maximum and median values of MD were significantly higher in patients with PD than in controls (both in separate lobes and the entire brain). We subsequently investigated the area under curve, sensitivity, specificity, and optimal cut-off values of the diffusion index for the entire cohort (Table 2). Figure 2 shows the ROC curves for the minimum, median, and maximum values of MD/FA for each parcellated brain region that showed a significant difference between PD patients and controls. The results of ROC analysis from AD and RD are shown in Fig. 3. In the entire cohort, the highest AUC was observed for the maximum MD in the ipsilateral middle temporal lobe (AUC = 85.0 %; optimal cut-off = 0.912 × 10^{-3} mm^2/sec). In FA, the largest AUC was 77.0 % in the cuneus when the maximum value was used. In contrast, the AUC for the basal ganglia varied from 50 % (median AD in the ipsilateral globus pallidus) to 73.7 % (median AD in the contralateral caudate).

Comparison of changes of in patients with Parkinson's disease and healthy controls

Regardless of disease severity, the inferior parietal gyrus was the region showing the more pronounced differences in the maximum values of diffusivity (changes in MD: 26.8 %; AD: 15.0 %; RD: 26.6 %, respectively). In contrast, the most significant change in FA was identified in the posterior cingulum (22.6 % in the median value of FA). Figure 4 plots the percentage changes of DTI in the cortical regions of PD patients that showed significant

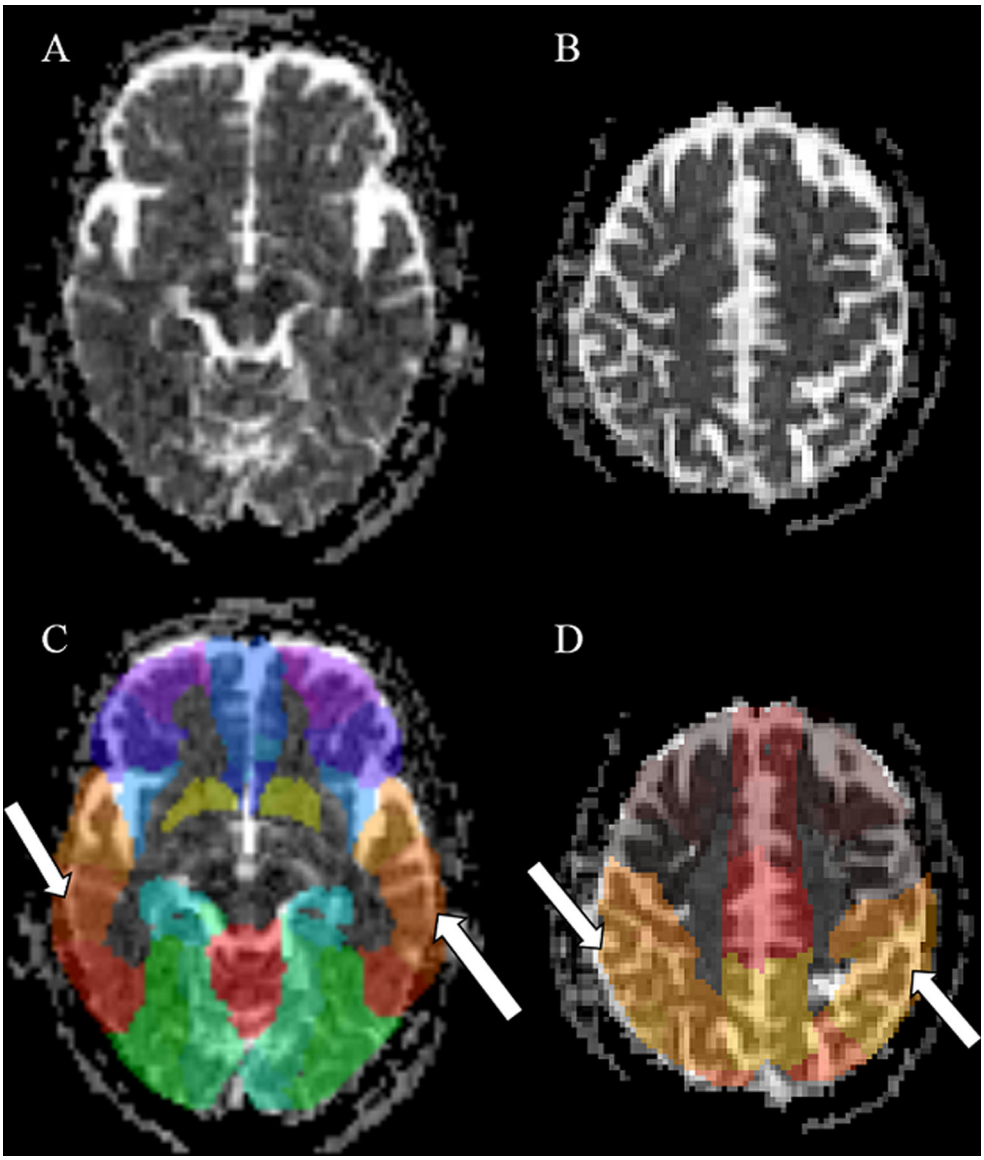

Fig. 1 Mean diffusivity from one representative patient. Two axial images of MD — located in the middle temporal lobe (*A*) and inferior parietal lobe (*B*) — from one representative patient are presented. The images were overlapped with the corresponding AAL template (*C* and *D*, respectively)

differences. The changes in the maximum values were more pronounced than those observed for median values. A lower number of regions with significant changes were detected when using minimum values. The median values of MD indicated that most of the ipsilateral occipital and parietal regions were affected, although the frontal regions were relatively spared.

Correlation of DTI with disease severity

After adjustment for disease duration, we found a statistically significant association between ADL and maximum MD/RD in the ipsilateral posterior cingulum (correlation coefficients = -0.421/-0.431). In the ipsilateral precuneus, we identified a significant association between ADL scores and median RD (correlation coefficient = -0.433). No significant associations were evident between the diffusion index and other clinical scores.

Effect of cerebral atrophy

In order to examine the extent of cerebral atrophy in the study patients, voxel-based morphometry was performed (Fig. 5). Only sparse changes at the frontal, parietal, and occipital regions were evident. However, more substantial changes were noted at caudate nucleus, midbrain (peri-aqueduct region), and peribasal cistern (anterior medial temporal lobe, amygdala) regions.

Table 1 Mean diffusivity values of the study participants

		MD		FA		AD		RD	
		Controls	PD	Controls	PD	Controls	PD	Controls	PD
Whole brain	Max	1.100 (0.290)	1.123 (0.265)	0.518 (0.109)	0.516 (0.110)	1.456 (0.247)	1.496 (0.233)	0.991 (0.282)	1.013 (0.256)
	Med	0.743 (0.066)	0.758 (0.073)	0.277 (0.065)	0.275 (0.066)	1.102 (0.081)	1.128 (0.092)	0.631 (0.077)	0.645 (0.084)
	Min	0.524 (0.083)	0.526 (0.084)	0.142 (0.034)	0.141 (0.034)	0.882 (0.066)	0.894 (0.070)	0.743 (0.066)	0.758 (0.073)
Frontal	Max	1.163 (0.287)	1.174 (0.253)	0.493 (0.075)	0.489 (0.076)	1.501 (0.226)	1.540 (0.204)	1.052 (0.275)	1.062 (0.237)
	Med	0.752 (0.046)	0.766 (0.053)	0.265 (0.036)	0.262 (0.036)	1.119 (0.050)	1.143 (0.063)	0.643 (0.051)	0.656 (0.057)
	Min	0.535 (0.060)	0.537 (0.061)	0.136 (0.019)	0.135 (0.020)	0.896 (0.051)	0.905 (0.056)	0.752 (0.046)	0.766 (0.053)
Parietal	Max	1.223 (0.326)	1.253 (0.313)	0.499 (0.061)	0.499 (0.065)	1.603 (0.268)	1.660 (0.269)	1.120 (0.310)	1.149 (0.295)
	Med	0.774 (0.056)	0.792 (0.066)	0.248 (0.033)	0.247 (0.034)	1.065 (0.067)	1.201 (0.085)	0.666 (0.064)	0.682 (0.073)
	Min	0.551 (0.054)	0.550 (0.060)	0.120 (0.015)	0.119 (0.015)	0.924 (0.042)	0.940 (0.046)	0.774 (0.056)	0.792 (0.066)
Occipital	Max	1.061 (0.156)	1.105 (0.165)	0.466 (0.067)	0.470 (0.068)	1.425 (0.112)	1.478 (0.134)	0.971 (0.142)	1.014 (0.149)
	Med	0.767 (0.036)	0.781 (0.042)	0.236 (0.031)	0.237 (0.034)	1.113 (0.044)	1.141 (0.055)	0.665 (0.045)	0.677 (0.051)
	Min	0.582 (0.040)	0.579 (0.046)	0.118 (0.012)	0.116 (0.013)	0.899 (0.033)	0.911 (0.038)	0.767 (0.036)	0.781 (0.042)
Temporal	Max	1.076 (0.251)	1.112 (0.231)	0.502 (0.075)	0.496 (0.076)	1.379 (0.193)	1.416 (0.168)	0.962 (0.241)	0.997 (0.220)
	Med	0.743 (0.048)	0.760 (0.056)	0.271 (0.040)	0.267 (0.040)	1.069 (0.052)	1.093 (0.062)	0.637 (0.053)	0.654 (0.060)
	Min	0.511 (0.060)	0.518 (0.063)	0.146 (0.023)	0.143 (0.022)	0.854 (0.044)	0.863 (0.051)	0.743 (0.048)	0.760 (0.056)
Other	Max	0.955 (0.302)	0.966 (0.251)	0.625 (0.157)	0.621 (0.159)	1.371 (0.301)	1.392 (0.264)	0.835 (0.300)	0.846 (0.249)
	Med	0.686 (0.091)	0.701 (0.100)	0.351 (0.093)	0.349 (0.095)	1.054 (0.118)	1.076 (0.128)	0.554 (0.104)	0.567 (0.112)
	Min	0.458 (0.120)	0.465 (0.124)	0.182 (0.046)	0.180 (0.045)	0.845 (0.097)	0.858 (0.102)	0.686 (0.091)	0.701 (0.100)

Diffusivity is expressed in 10^{-3} mm^2/sec. Average values are reported for the entire brain and different lobes. Data are reported as means (standard deviations). *MD* mean diffusivity, *FA* fractional anisotropy, *RD* radial diffusivity, *AD* axial diffusivity, *PD* Parkinson's disease. *Max* maximum, *Med* median, *Min* minimum

Table 2 Results of receiver operating characteristic (ROC) analysis of mean diffusivity values

Regions		Area under curve	Optimal cut-off value	Sensitivity	Specificity
MD					
Minimum	Ipsi_ParaHippocampal	0.681	0.494	0.643	0.692
Median	Cont_Calcarine	0.799	0.766	0.754	0.758
Maximum	Ipsi_Temporal_Mid	0.850	0.912	0.706	0.857
FA					
Minimum	Ipsi_Cingulum_Post	0.673	0.187	0.349	0.967
Median	Ipsi_Calcarine	0.743	0.220	0.619	0.846
Maximum	Ipsi_Cuneus	0.770	0.465	0.579	0.846
AD					
Minimum	Ipsi_Calcarine	0.787	0.910	0.579	0.890
Median	Ipsi_Angular	0.790	1.140	0.786	0.714
Maximum	Ipsi_Angular	0.827	1.445	0.690	0.824
RD					
Minimum	Ipsi_ParaHippocampal	0.690	0.365	0.603	0.758
Median	Cont_Calcarine	0.777	0.652	0.595	0.868
Maximum	Ipsi_Temporal_Mid	0.843	0.817	0.754	0.802

The results of ROC analysis are expressed using the area under the ROC curve, the optimal cut-off points, and the corresponding sensitivity and specificity values. The diffusivity values are expressed in 10^{-3} mm^2/sec. (*MD* mean diffusivity, *FA* fractional anisotropy, *AD* axial diffusivity, *RD* radial diffusivity)

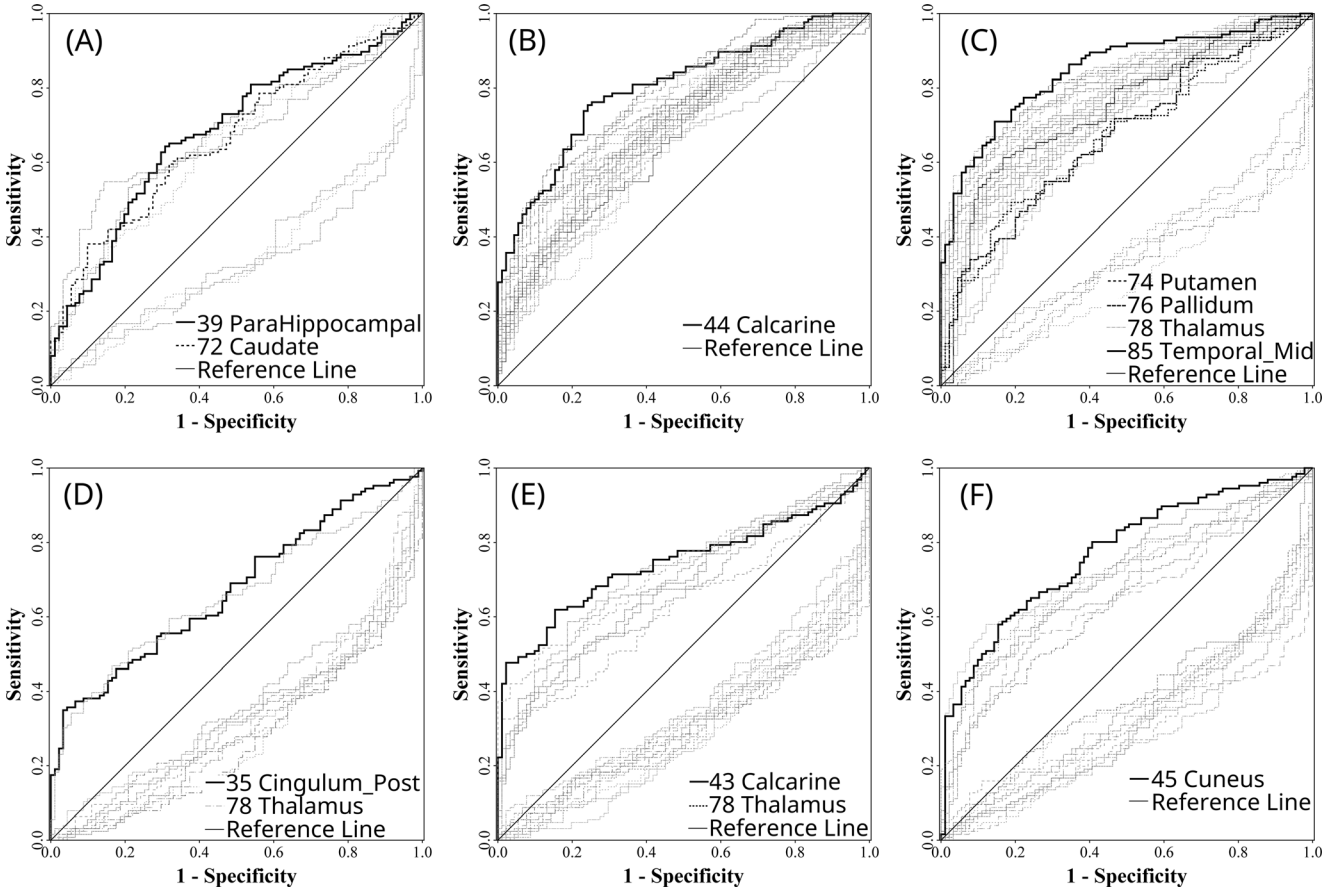

Fig. 2 Receiver operating characteristic analysis of mean diffusivity and fractional anisotropy. The figure depicts the receiver operating characteristic curves for mean diffusivity (*top*) and fractional anisotropy (*bottom*). *A*, *D*: minimum; *B*, *E*: median; *C*, *F*: maximum, respectively. Curves from the striatum or showing the largest area are highlighted in *bold*. The labelling for the rest of the curves was in supplementary Figure 1

Discussion

There are two principal findings in this study. First, MD was significantly higher in PD patients than in controls. Notably, such differences extended beyond the basal ganglia. The ipsilateral inferior parietal gyrus was the site showing the most significant change in MD. Secondly, we identified a distinct spatial pattern of diffusion change in terms of the affected cortical regions. The automatic parcellation procedure does not require the manual definition of the region of interest, which is subjective and tedious.

Conventional anatomical MRI typically yields negative findings in terms of volume measurement in patients with PD [27]. In this regard, no significant volumetric differences in total brain, caudate, or substantia nigra were detected, the only exception being a reduced pallidal volume in patients with advanced disease [28]. Taken together, these results suggest that volumetry cannot serve as a diagnostic tool. Although the diagnosis of PD continues to be based on clinical manifestations, MRI is frequently prescribed in patients with suspected PD to rule out the presence of concomitant neurological diseases. Nuclear medicine examinations (e.g., Trodat imaging) may also be used to increase the diagnostic confidence. Based on the increased AUC, DTI may potentially be useful for diagnostic purposes. We speculate that the use of this imaging modality may be cost-effective and reduce the time and expenses related to repeated clinical examinations.

Largest AUC and DTI-related changes

Diffusivity was significantly higher in PD patients than in controls. Notably, we also demonstrated a specific cortical involvement which extended beyond basal ganglia and might involve the visual area. Although basal ganglia are the regions that play the major role in the pathophysiology of PD, here we have shown that DTI values in these regions have a limited AUC. The maximum values of water diffusivity had a higher diagnostic accuracy than traditionally used mean values. The regions with the highest AUC were different among different diffusion indices, including calcarine, cuneus, angular, parahippocampus, and posterior cingulum. The best AUC can be as high as 85.0 % (the maximum MD of the ipsilateral middle temporal lobe). When compared with normal controls, the maximum values of MD, AD, and RD concordantly identified the ipsilateral inferior parietal gyrus as the region with the most significant change. Both the maximum values of MD

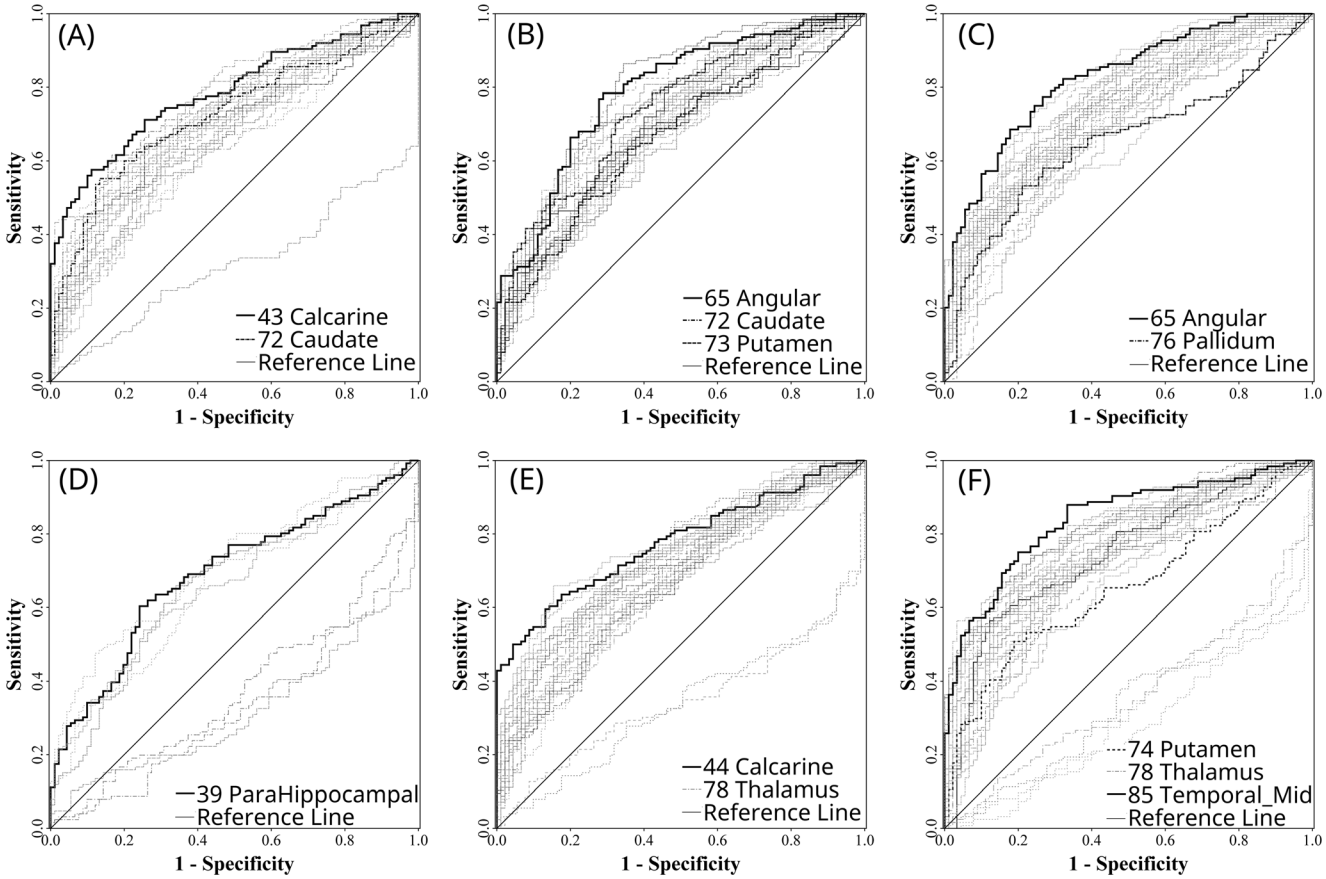

Fig. 3 Receiver operating characteristic analysis of axial and radial diffusivities. The figure depicts the receiver operating characteristic curves for axial (*top*) and radial diffusivity. *A*, *D*: minimum; *B*, *E*: median; *C*, *F*: maximum, respectively. Curves from the striatum or showing the largest area are highlighted in *bold* The labelling for the rest of the curves was in supplementary Figure 2

and RD from the ipsilateral posterior cingulum showed a significant correlation with ADL.

The impairment of these regions in PD may reflect the loss of dopaminergic inputs from the midbrain. The dysfunction in the inferior parietal lobule and middle temporal lobes has been linked to memory [29, 30] or motor [31, 32] deficits in PD patients. A metabolic impairment of the cingulate cortex has been also reported in PD [16]. Interestingly, the observed increased MD in the middle temporal gyrus and inferior parietal lobe might be in broad agreement with the Braak's pathological staging. In patients with advanced PD, an involvement of the anteromedial temporal mesocortex (that receives afferents from the sensory association areas of the parietal, occipital, and temporal neocortices) is common [33]. We, thus, believe that our observations may be useful for understanding the neuroanatomical basis of memory or cognitive dysfunction in late-stage PD and dopamine agonist-induced impulse control disorders. Our data suggest that structural alterations in the cortical brain (detected by DTI) may have a key role in the aetiology of PD.

Additional DTI metrics and the use of the maximum values

Although no significant directional preference exists for water diffusion within gray matter, the values of FA, AD, and RD identified in the current study had a potential diagnostic capacity. Fractional anisotropy was found to be increased in some cortical areas and decreased in other regions. Such discrepancies may explain, at least in part, the inconsistencies previously reported in DTI studies focusing on PD patients. Unfortunately, a universally accepted model for quantifying DTI changes at the gray matter level is still lacking. We believe that our data may serve for future reference and can prompt further studies on PD with the advance of diffusion MRI [34, 35].

The maximum values of MD had a higher AUC than traditionally used mean values. Controversy still exists regarding the potential changes of MD measured in the basal ganglia of patients with PD [13]. Notably, noise distribution intrinsic to DTI measurements and the use of a parcellation method may result in either overestimation or underestimation of MD. To circumvent this issue, we performed all analyses separately for

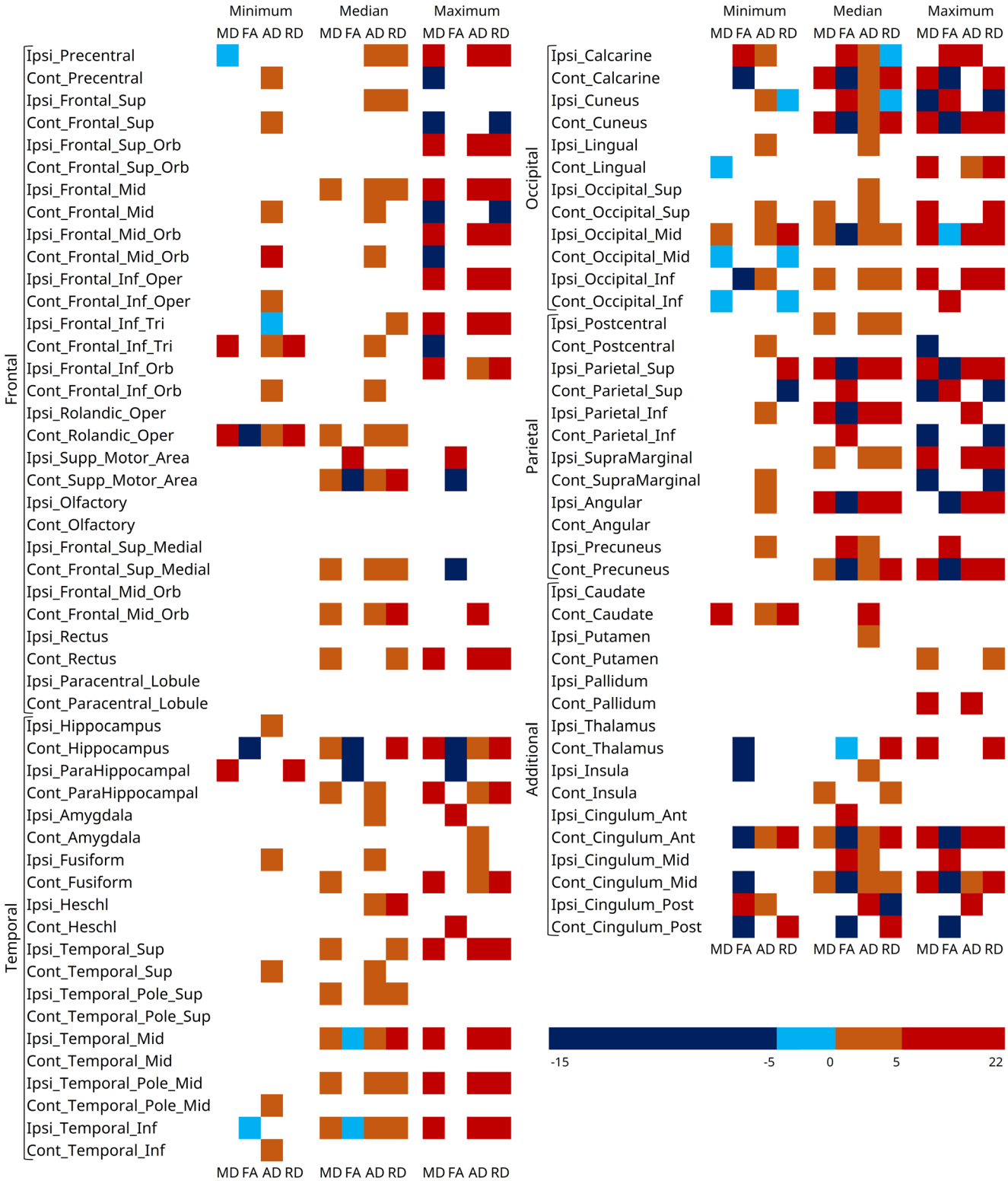

Fig. 4 Changes of diffusion index from the parcellated brain regions. The figure displays the percentage change of diffusion tensor for parcellated brain regions characterized by the presence of statistically significant differences between PD patients and healthy controls (in the frontal, occipital, parietal, temporal and additional areas, respectively)

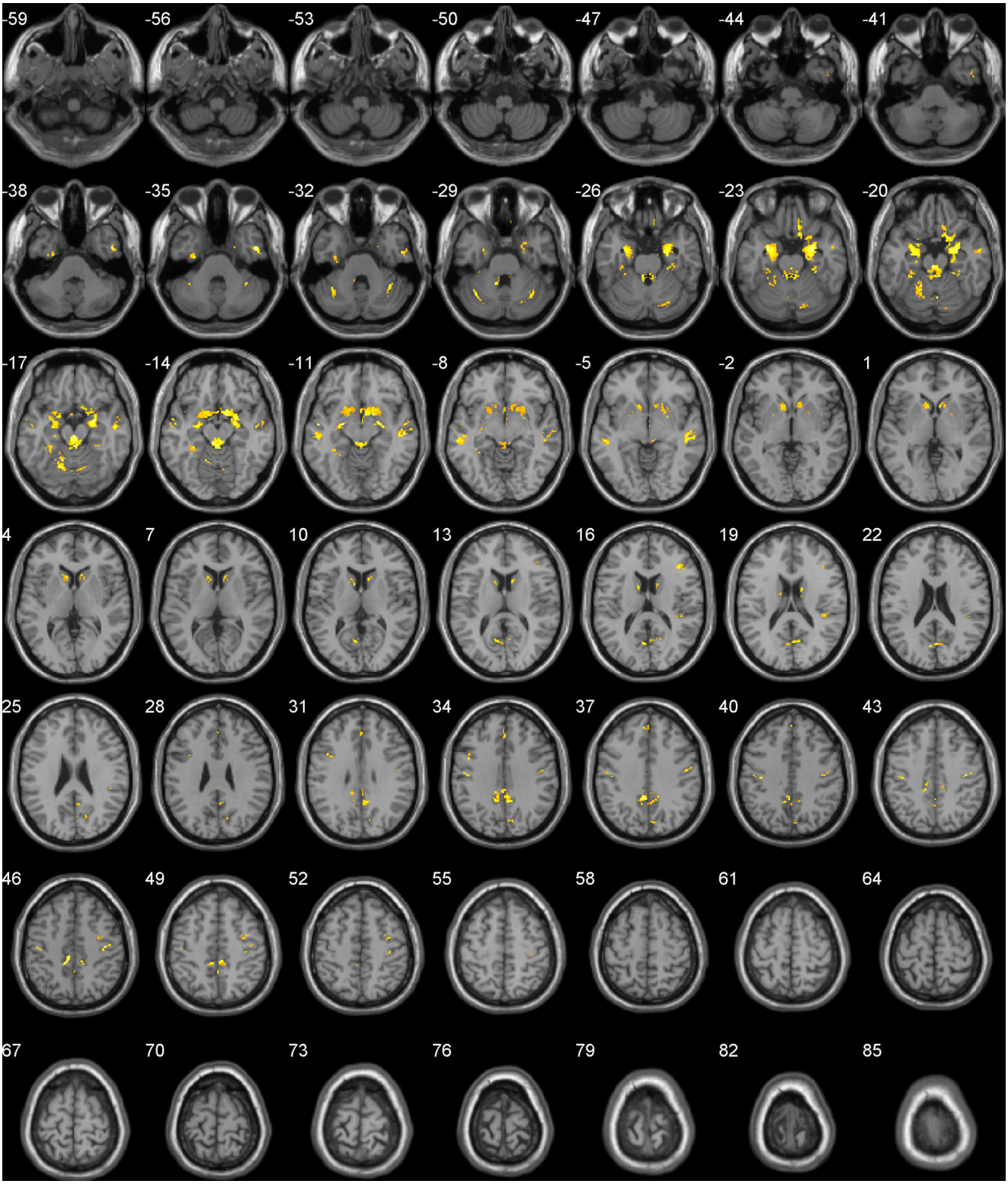

Fig. 5 Voxel-based morphometry. The figure shows the results of voxel-based morphometry. Compared with healthy controls, the atrophy identified in patients is highlighted in *colour* and overlapped with high-resolution T1 images. Only sparse changes in the cortical regions were evident

the 10th (minimum), 50th (median), and 90th (maximum) percentiles of MD. The results indicated that maximum MD allowed identifying a higher number of affected brain areas compared with median and minimum values. Consequently,

the use of maximum MD should be strongly recommended in future DTI studies focusing on PD.

The interpretation of DTI changes

The measured apparent diffusion coefficient can result from both intra- and extra-cellular contributions. Because the diffusivity from the extracellular water is larger, the increase in apparent diffusion is frequently related to an increased extracellular space. In general, an increased extracellular diffusion can reflect an increased cell membrane permeability (e.g., as a result of cell death). An increased MD is frequently attributed to a loss of water balance in the microstructural environment, possibly related to cellular degeneration, demyelination, or axonal loss [36]. Therefore, the measured maximum MD might reflect a significant contribution from the extracellular space (and chiefly from the CSF). In this scenario, it is conceivable that the maximum MD may be superior to traditional median MD data for detecting pathological brain changes. Notably, MD was not invariably increased in all of our PD patients. In this regard, the use of minimum MD did not allow identifying brain regions with significant differences.

Patients with early-stage PD typically have unilateral symptoms. In the current study, regions characterized by significant increase of MD could be either unilateral or bilateral. The regions showing the highest AUC (ipsilateral middle temporal gyrus) and the most significant signal change (ipsilateral inferior parietal gyrus) were both ipsilateral. Such ipsilateral increases of MD are consistent with a previous MR spectroscopy study [37] and have been attributed to unilateral neuronal dysfunction. Further investigations are needed to shed more light on this issue.

Effect of cerebrospinal fluid

In PD, cerebral atrophy has been reported in various areas [29, 38, 39]. In the presence of cerebral atrophy, CSF contamination might result in an increased MD. Furthermore, a 2 × 2 × 3-mm^3 resolution for the diffusion measurement is poor, albeit being commonly used in DTI studies of the human brain. These factors may potentially result in deteriorated partial volume effects on gray matter. In order to reduce the potential confounding impact of CSF, images were segmented during the post-processing phase and only segmented gray matter was used for the analysis. Notably, only sparse changes at the frontal, parietal, and occipital regions were noted, exerting only minimal or no contribution to diffusion index alterations in such areas. Because we cannot completely rule out the potential confounding effect of CSF, caution should be exercised in the interpretation of our findings.

Study limitations and future directions

DTI is commonly used for imaging the white matter. In this regard, the modelling of the axial and radial diffusivities along and across the neuron fibre tracts used in this study may be problematic because no such structures exist in the gray matter. Moreover, changes in the two indices for regions characterized by a low directionality are difficult to interpret (29). The involvement of the frontal and temporal lobes observed herein suggests the involvement of these regions in the alterations of executive functions, emotions, language, and memory frequently observed in patients with severe PD [40]. Our findings may prompt further investigations of quantitative DTI-derived biomarkers in PD patients, potentially accelerating their clinical adoption in this common neurodegenerative disorder. Further DTI studies are also required to investigate the associations of the potentially impaired cognitive functions and dementia in patients with PD.

Conclusions

Diffusion tensor imaging detected significant changes in the parcellated cerebral regions of patients with PD and has an AUC as high as 85.0 % from the middle temporal lobe. Our pilot results suggest the potential diagnostic utility of measuring the maximum value of MD in PD patients, with a satisfactory diagnostic sensitivity and specificity.

Acknowledgements The scientific guarantor of this publication is Jiun-Jie Wang. The authors of this manuscript declare no relationships with any companies whose products or services may be related to the subject matter of the article. This study has received funding by the Ministry of Science and Technology Taiwan (103-2325-B-182-001 and 104-2314-B-182-042) and the Chang-Gung Memorial Hospital (CMRPD3D0011-3, CIRPD1E0061 and CMRPD1C0291-3). One of the authors has significant statistical expertise. Institutional review board approval was obtained. Written informed consent was obtained from all subjects (including patients) in this study. Some study subjects or cohorts have been previously reported in (10.3389/fnagi.2013.00071). 77 healthy controls have been previously reported (10.3389/fnagi.2013.00071). The prior article discussed the change of water diffusion in the ageing process whereas this manuscript focused on the diagnosis of Parkinson's disease.

Methodology: prospective, case-control study, performed at one institution.

The imaging facility was supported by the Imaging Core Laboratory of Institute for Radiological Research and Center for Advanced Molecular Imaging and Translation. The authors would like to thank the Neuroscience Research Center, Chang Gung Memorial Hospital, Imaging Core Laboratory of Institute for Radiological Research, Chang Gung University/Chang Gung Memorial Hospital, Linkou and the Healthy Aging Research Center, Chang Gung University for providing support. The funding source had no involvement in the collection, analysis, and interpretation data; in the writing of the report; and in the decision to submit the paper for publication.

References

1. Lang AE, Lozano AM (1998) Parkinson's disease. First of two parts. N Engl J Med 339:1044–1053
2. Lang AE, Lozano AM (1998) Parkinson's disease. Second of two parts. N Engl J Med 339:1130–1143
3. Adler CH, Beach TG, Hentz JG et al (2014) Low clinical diagnostic accuracy of early vs advanced Parkinson disease: clinicopathologic study. Neurology 83:406–412
4. Tessitore A, Amboni M, Cirillo G et al (2012) Regional gray matter atrophy in patients with Parkinson disease and freezing of gait. AJNR Am J Neuroradiol 33:1804–1809
5. Choi SH, Jung TM, Lee JE, Lee SK, Sohn YH, Lee PH (2012) Volumetric analysis of the substantia innominata in patients with Parkinson's disease according to cognitive status. Neurobiol Aging 33:1265–1272
6. Carlesimo GA, Piras F, Assogna F, Pontieri FE, Caltagirone C, Spalletta G (2012) Hippocampal abnormalities and memory deficits in Parkinson disease: a multimodal imaging study. Neurology 78: 1939–1945
7. Chang CC, Chang WN, Lui CC et al (2011) Clinical significance of the pallidoreticular pathway in patients with carbon monoxide intoxication. Brain 134:3632–3646
8. Wang J, Wai Y, Lin WY et al (2010) Microstructural changes in patients with progressive supranuclear palsy: a diffusion tensor imaging study. J Magn Reson Imaging 32:69–75
9. Menke RA, Scholz J, Miller KL et al (2009) MRI characteristics of the substantia nigra in Parkinson's disease: a combined quantitative T1 and DTI study. NeuroImage 47:435–441
10. Karagulle Kendi AT, Lehericy S, Luciana M, Ugurbil K, Tuite P (2008) Altered diffusion in the frontal lobe in Parkinson disease. AJNR Am J Neuroradiol 29:501–505
11. Zhang Y, Schuff N, Jahng GH et al (2007) Diffusion tensor imaging of cingulum fibers in mild cognitive impairment and Alzheimer disease. Neurology 68:13–19
12. Acosta-Cabronero J, Alley S, Williams GB, Pengas G, Nestor PJ (2012) Diffusion tensor metrics as biomarkers in Alzheimer's disease. PLoS One 7, e49072
13. Gattellaro G, Minati L, Grisoli M et al (2009) White matter involvement in idiopathic Parkinson disease: a diffusion tensor imaging study. AJNR Am J Neuroradiol 30:1222–1226
14. Vaillancourt DE, Spraker MB, Prodoehl J et al (2009) High-resolution diffusion tensor imaging in the substantia nigra of de novo Parkinson disease. Neurology 72:1378–1384
15. Cochrane CJ, Ebmeier KP (2013) Diffusion tensor imaging in parkinsonian syndromes: a systematic review and meta-analysis. Neurology 80:857–864
16. Kikuchi A, Baba T, Hasegawa T et al (2013) Hypometabolism in the supplementary and anterior cingulate cortices is related to dysphagia in Parkinson's disease: a cross-sectional and 3-year longitudinal cohort study. BMJ open 3
17. Chan LL, Rumpel H, Yap K et al (2007) Case control study of diffusion tensor imaging in Parkinson's disease. J Neurol Neurosurg Psychiatry 78:1383–1386
18. Chen Z, Ma L, Lou X, Zhou Z (2010) Diagnostic value of minimum apparent diffusion coefficient values in prediction of neuroepithelial tumor grading. J Magn Reson Imaging 31:1331–1338
19. Murakami R, Hirai T, Sugahara T et al (2009) Grading astrocytic tumors by using apparent diffusion coefficient parameters: superiority of a one- versus two-parameter pilot method. Radiology 251: 838–845
20. Lo CY, Wang PN, Chou KH, Wang J, He Y, Lin CP (2010) Diffusion tensor tractography reveals abnormal topological organization in structural cortical networks in Alzheimer's disease. J Neurosci Off J Soc Neurosci 30:16876–16885
21. Ng SH, Hsu WC, Wai YY et al (2013) Sex dimorphism of cortical water diffusion in normal aging measured by magnetic resonance imaging. Front Aging Neurosci 5:71
22. Alexander DC, Pierpaoli C, Basser PJ, Gee JC (2001) Spatial transformations of diffusion tensor magnetic resonance images. IEEE Trans Med Imaging 20:1131–1139
23. Modrego PJ, Fayed N, Artal J, Olmos S (2011) Correlation of findings in advanced MRI techniques with global severity scales in patients with Parkinson disease. Acad Radiol 18:235–241
24. Litvan I, Bhatia KP, Burn DJ et al (2003) SIC task force appraisal of clinical diagnostic criteria for parkinsonian disorders. Mov Disord 18:467–486
25. Ashburner J, Friston KJ (2000) Voxel-based morphometry–the methods. NeuroImage 11:805–821
26. Cook PA, Bai Y, Nedjati-Gilani S, Seunarine KK, Hall MG, Parker GJ, Alexander DC (2006) Camino: open-source diffusion-mri reconstruction and processing 14th scientific meeting of the International Society for Magnetic Resonance in Medicine, Seattle, WA, USA, p 2759
27. Schulz JB, Skalej M, Wedekind D et al (1999) Magnetic resonance imaging-based volumetry differentiates idiopathic Parkinson's syndrome from multiple system atrophy and progressive supranuclear palsy. Ann Neurol 45:65–74
28. Geng DY, Li YX, Zee CS (2006) Magnetic resonance imaging-based volumetric analysis of basal ganglia nuclei and substantia nigra in patients with Parkinson's disease. Neurosurgery 58:256–262, **discussion 256–262**
29. Burton EJ, McKeith IG, Burn DJ, Williams ED, O'Brien JT (2004) Cerebral atrophy in Parkinson's disease with and without dementia: a comparison with Alzheimer's disease, dementia with Lewy bodies and controls. Brain 127:791–800
30. Gonzalez-Redondo R, Garcia-Garcia D, Clavero P et al (2014) Grey matter hypometabolism and atrophy in Parkinson's disease with cognitive impairment: a two-step process. Brain 137:2356–2367
31. Cunnington R, Egan GF, O'Sullivan JD, Hughes AJ, Bradshaw JL, Colebatch JG (2001) Motor imagery in Parkinson's disease: a PET study. Mov Disord 16:849–857
32. Matsui H, Udaka F, Miyoshi T et al (2006) Frontal assessment battery and brain perfusion image in Parkinson's disease. J Geriatr Psychiatry Neurol 19:41–45
33. Braak H, Del Tredici K (2008) Invited Article: Nervous system pathology in sporadic Parkinson disease. Neurology 70:1916–1925
34. Zhang H, Schneider T, Wheeler-Kingshott CA, Alexander DC (2012) NODDI: practical in vivo neurite orientation dispersion and density imaging of the human brain. NeuroImage 61:1000–1016
35. Jensen JH, Helpern JA (2010) MRI quantification of non-Gaussian water diffusion by kurtosis analysis. NMR Biomed 23:698–710
36. Basser PJ, Pierpaoli C (1996) Microstructural and physiological features of tissues elucidated by quantitative-diffusion-tensor MRI. J Magn Reson B 111:209–219
37. Choe BY, Park JW, Lee KS et al (1998) Neuronal laterality in Parkinson's disease with unilateral symptom by in vivo 1H magnetic resonance spectroscopy. Investig Radiol 33:450–455
38. Lyoo CH, Ryu YH, Lee MS (2010) Topographical distribution of cerebral cortical thinning in patients with mild Parkinson's disease without dementia. Mov Disord 25:496–499
39. Summerfield C, Junque C, Tolosa E et al (2005) Structural brain changes in Parkinson disease with dementia: a voxel-based morphometry study. Arch Neurol 62:281–285
40. Aarsland D, Andersen K, Larsen JP, Lolk A, Nielsen H, Kragh-Sorensen P (2001) Risk of dementia in Parkinson's disease: a community-based, prospective study. Neurology 56:730–736